Journal of Magnetic Resonance **140,** 200–205 (1999)
Article ID jmre.1999.1793, available online at http://www.idealibrary.com on IDEAL®

Multiple Echoes, Multiple Quantum Coherence, and the Dipolar Field: Demonstrating the Significance of Higher Order Terms in the Equilibrium Density Matrix

E. D. Minot, P. T. Callaghan, and N. Kaplan*

Institute of Fundamental Sciences–Physics, Massey University, Palmerston North, 11222, New Zealand; and
**Racah Institute of Physics, Hebrew University of Jerusalem, Jerusalem, Israel*

Received January 22, 1999; revised April 27, 1999

It is well known that dipolar field effects lead to multiple spin echoes in a simple two-RF pulse experiment (the MSE experiment). We show here that coherence transfer echoes (which identify the existence of multiple quantum coherences in liquid NMR) and multiple spin echoes have a common origin. Using density matrix theory we have calculated the phase and timing of multiple spin echoes from all quadrature phase combinations of RF pulses. We show for the MSE experiment that there is a one-to-one correspondence between the time domain echo order and the multiple quantum coherence order. The experimental confirmation of these phase predictions shows that multiple spin echoes provide independent evidence for the breakdown of the high temperature approximation as proposed by Warren *et al.* (*Science* 262, 2005 (1993)).

INTRODUCTION

It is well known that in samples with large magnetization density, the dipolar field causes nonlinearities in the Bloch equations and hence complex time evolution of spin magnetization, in particular the appearance of multiple echoes following a simple two-RF pulse spin-echo sequence (*1–4*). In 1993 Warren and co-workers demonstrated that these nonlinear effects and their description had much in common with multiple quantum coherence phenomena found in high-resolution NMR experiments in which bilinear terms in the spin Hamiltonian provide the means to explore different coherence pathways. In particular Warren simplified the description of these complex phenomena by demonstrating that they may be understood by considering the evolution of the spin density matrix in the dipolar field (*5, 6*). A key ingredient of the physics is the existence of high-order terms in the equilibrium density matrix. The breakdown of the usual high temperature approximation (HTA) is central to Warren's description. The assertion of HTA breakdown is controversial and there exists some uncertainty as to whether the effects of classical nonlinearities and such quantum order phenomena really are one and the same. Recently Jeener *et al.* (*7*), Levitt (*8*), and Warren *et al.* (*9*) have published important theoretical arguments showing that indeed they are.

Here we provide a simple experimental demonstration that such higher order terms must exist in the equilibrium density matrix. We further make clear the relationship between these terms, the existence of multiple quantum coherences as identified in coherence transfer echoes (the CRAZED experiment), and the multiple echoes which occur in the time domain following a simple two-pulse experiment involving 90° RF pulses. In particular we show here that there is a one-to-one correspondence between the time domain echo order and the multiple quantum coherence order.

We recognize that most of the ideas contained in this note are inherent in the work of Warren and co-authors. However the particular experimental results which we describe here have not, to our knowledge, been reported previously. Furthermore we believe that our results have pedagogic value. First, they provide independent evidence for the equilibrium density matrix description of Warren *et al.* Second, they help elucidate the relationship between the multiple echo experiment (*1–4*) and the CRAZED experiment (*5*). Third, they provide a practical demonstration of how these various coherences can be manipulated.

THEORY OF THE MULTIPLE SPIN ECHO (MSE) AND CRAZED EXPERIMENTS

Figure 1a shows a simple two-RF pulse experiment in which the spins are immersed in a steady magnetic field gradient. This experiment has been shown to generate multiple echoes, provided that the equilibrium spin magnetization is sufficiently large. In particular these effects are seen in ^{3}He NMR experiments performed at low temperatures (*1, 2*), or in ^{1}H NMR experiments in water placed in a high-field superconducting magnet (*3, 4*). Figure 1b shows the CRAZED experiment (correlated spectroscopy sequence revamped with asymmetric z-gradient echo detection) of Warren *et al.* (*5*) in which the background gradients are minimized (in order to perform high-resolution NMR spectroscopy) but a pair of gradient pulses are applied in order to select desired spin coherences. This experiment is performed in two dimensions, t_1 being the evolution

1090-7807/99 $30.00

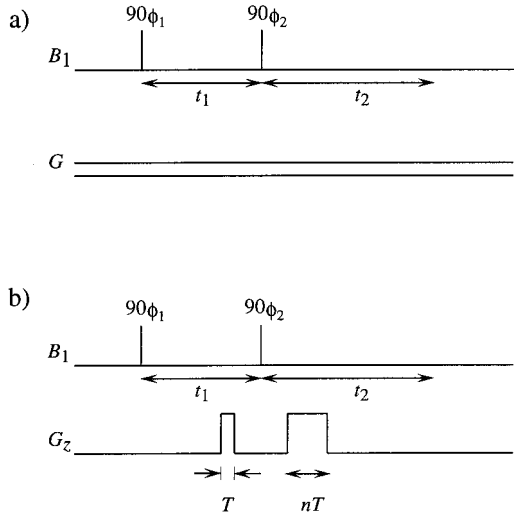

FIG. 1. (a) The MSE experiment. ϕ_1 and ϕ_2 denote the phase of the RF pulses. G is a steady background gradient in the z direction unless otherwise stated. The MSE signals occur at $t_2 = t_1, 2t_1, 3t_1 \cdots$ (b) The nth-order CRAZED experiment. T is the period of the first gradient pulse, $n = 1, 2, 3 \cdots$. The CRAZED signal occurs at $t_2 = nt_1$.

dimension, and t_2 the acquisition dimension. Coherence selection relies on relative Larmor precession. For example, when the area under the second gradient pulse is twice that under the first ($n = 2$ in Fig. 1b), the subsequent signal (and hence transverse magnetization) with Larmor frequency ω in the t_2 domain must have originated from coherences whose Larmor frequencies were 2ω during t_1. The fact that the CRAZED experiment indicates the existence of double-quantum coherence during t_1 provides powerful evidence that second-order terms must exist in the spin density matrix even before the application of the first RF pulse.

A complete treatment of the density matrix description of the CRAZED experiment has been given by Warren *et al.* (*6*). Here we reproduce the essential details, showing in addition how it predicts the character of various echo orders of the MSE experiment (Fig. 1a), including the timing and phase of each echo. This theoretical development will be important later in our discussion where we develop and demonstrate a phase cycle which can be used to select echo orders at will. In the energy representation the thermal equilibrium density matrix may be written

$$\rho_{\text{eq}} = \frac{\exp(-\beta\mathcal{H})}{\text{Tr}(\exp(-\beta\mathcal{H}))}, \qquad [1]$$

where $\beta = 1/k_{\text{B}}T$. In the case of an N-spin system of coupled spin-$\frac{1}{2}$ particles, $\mathcal{H}$ is a $2^N \times 2^N$ matrix and is given by

$$\mathcal{H} = \sum_i^N \hbar\omega_i I_{zi} + \sum_{i,j}^N \hbar D_{ij} I_{zi} I_{zj}, \qquad [2]$$

where D_{ij} is the dipolar coupling between spins i and j and ω_i is the resonant frequency of the ith spin. Equation [2] does not include all secular terms from the dipolar interaction Hamiltonian (*10*); however, we are concerned with the formation of multiple echoes and these are due to the $I_{zi}I_{zj}$ terms. In solids the sum of dipolar coupling terms for the ith spin is generally 10^4 smaller than the Zeeman term and in liquids some further 10^4 lower due to motional averaging. Thus dipolar interactions can be ignored as far as the composition of the equilibrium density matrix is concerned. Normally, it is sufficient to use a single spin picture when calculating the equilibrium magnetization, so that for nuclear spins in the presence of a Zeeman Hamiltonian $\mathcal{H} = -\hbar\omega_i I_{zi}$, the HTA ($\beta\hbar\omega_i \ll 1$) gives, for the single spin-$\frac{1}{2}$ density matrix,

$$\sigma_{\text{eq}} \approx \tfrac{1}{2}(\mathbf{1} + \beta\hbar\omega_i I_z), \qquad [3]$$

where **1** is the identity matrix. We have used the expansion for the Brillouin function $\tanh(\beta\hbar\omega_i) \approx \beta\hbar\omega_i$. For the N spin system the density matrix becomes

$$\begin{aligned}\rho_{\text{eq}} &= \sigma_{1\text{eq}} \otimes \sigma_{2\text{eq}} \otimes \sigma_{3\text{eq}} \cdots \otimes \sigma_{N\text{eq}} \\ &= 2^{-N}\Pi_i(\mathbf{1} + \beta\hbar\omega_i I_{zi}),\end{aligned} \qquad [4]$$

which involves N one-spin operators of the form $\beta\hbar\omega_0 I_{zi}$ ($\omega_i \approx \omega_0 = \gamma B_0$), $N^2/2$ two-spin operators $(\beta\hbar\omega_0)^2 I_{zi}I_{zj}$, and higher order spin operators in succession. The increasing multiplicity of higher order terms by successive powers of N means that higher order terms in ρ_{eq} cannot be ignored without further justification. In conventional NMR experiments the justification for retaining only first-order terms is as follows. Consider a two-spin component of ρ_{eq}, $I_{zi}I_{zj}$, which is converted to $I_{yi}I_{yj}$ by a 90° RF pulse (taken to be of the form $\omega_1 I_x$). All subsequent Zeeman interactions produce density matrix terms which remain bilinear and so, cannot result in the NMR observables, I_x or I_y. Only the first-order terms of the equilibrium density matrix, $\beta\hbar\omega_0 I_{zi}$, lead to observable signal. When the effects of the dipolar field are considered the situation is somewhat altered.

Two important points are made by Warren *et al.* First, despite $\beta\hbar\omega_0$ being small (on the order of 10^{-4} for protons in 10 T), the large value of N ensures that the higher order terms do not vanish in ρ_{eq}, whether they become directly observable or not. Second, in order to become observable, there must exist in the spin Hamiltonian terms bilinear in the spin operators (i.e., of the form $I_{zi}I_{zj}$) over all density matrix pairs i, j which are to be refocused. Clearly a local scalar interaction cannot meet this second criterion. By contrast the dipolar field Hamiltonian which arises from an integral of all pairwise dipolar interactions between distant spins can suffice. In particular, Warren notes that while molecular self-diffusion in liquids causes dipolar interactions to be averaged to zero for spins on nearby molecules, beyond the diffusion length corresponding

to the characteristic NMR timescale ($r_{\min} \sim 10\ \mu$m), such averaging does not apply and the volume integral of $r^2 dr$ over the r^{-3} dependence of the dipolar interaction ensures a logarithmic contribution whose magnitude depends on the ratio of the sample dimension to the diffusion length. Of course, in a spherical sample the angular dependence of the dipolar interaction ensures that the dipolar field vanishes. However, if the spherical symmetry is broken, for example, by application of a magnetic field gradient, **G**, then the effects of the dipolar field will be felt by the spins and the conversion of higher order coherences into observable magnetization becomes possible.

Consider the two 90° RF pulse sequence shown in Fig. 1a. The gradient and dipolar interaction play no role in making a signal observable from ρ terms linear in I_z. This signal is the primary echo in an MSE experiment which occurs at $t_2 = t_1$. We shall begin by considering the evolution of an element of the second-order ρ_{eq} term, $(\beta\hbar\omega_0)^2 I_{zi} I_{zj}$. Ignoring the effects of spin–spin relaxation, it is a straightforward exercise (*11*) to show that it is first converted via the 90_x pulse to a term of order $I_{yi} I_{yj}$, then via the Zeeman and dipolar interactions to

$$\begin{aligned}\rho(t_{1-}) = \cos^2(D_{ij}t_1)[&I_{yi}I_{yj}\cos(\omega_i t_1)\cos(\omega_j t_1) \\ &+ I_{xi}I_{yj}\sin(\omega_i t_1)\cos(\omega_j t_1) + I_{yi}I_{xj}\cos(\omega_i t_1) \\ &\times \sin(\omega_j t_1) + I_{xi}I_{xj}\sin(\omega_i t_1)\sin(\omega_j t_1)] \\ &+ \sin(D_{ij}t_1)[\cdots].\end{aligned} \quad [5]$$

The second 90_x RF pulse then converts $\rho(t_{1-})$ to

$$\begin{aligned}\rho(t_{1+}) = \cos^2(D_{ij}t_1)[&I_{zi}I_{zj}\cos(\omega_i t_1)\cos(\omega_j t_1) \\ &+ I_{xi}I_{zj}\sin(\omega_i t_1)\cos(\omega_j t_1) + I_{zi}I_{xj}\cos(\omega_i t_1) \\ &\times \sin(\omega_j t_1) + I_{xi}I_{xj}\sin(\omega_i t_1)\sin(\omega_j t_1)] \\ &+ \sin(D_{ij}t_1)[\cdots].\end{aligned} \quad [6]$$

Completing the calculation of the evolution in the t_2 domain leads to over a hundred different density matrix terms, each with a different temporal modulation. However, only some of these many terms will generate observable coherences of the form I_x and I_y. We easily pick these terms since only terms of the form $I_{xi}[I_{zj}I_{zj}\cdots]$ or $I_{yi}[I_{zj}I_{zj}\cdots]$ evolve into transverse magnetization under the dipole Hamiltonian (*6*). In particular, the transverse magnetization at t_2 from the $n = 2$ pathway is

$$\begin{aligned}\sum_{i=1}^{N}\sum_{j=1}^{N} \sin(D_{ij}t_2)\cos^2(D_{ij}t_1)[&-I_{yi}\sin(\omega_i t_1)\sin(\omega_j t_1)\cos(\omega_i t_2) \\ &+ I_{xi}\sin(\omega_i t_1)\cos(\omega_j t_1)\sin(\omega_i t_2)].\end{aligned} \quad [7]$$

Terms that have more than one $\sin(D_{ij}t)(\approx D_{ij}t)$ factor are neglected here due to the weak dipolar interaction strength, i.e., $D_{ij}t_1,\ D_{ij}t_2 \ll 1$. Using the standard trigonometric identities one can factorize Expression [7] into terms which are a function of $\omega_i + \omega_j$ and $\omega_i - \omega_j$. Now we may understand the role of the applied magnetic field gradient which causes spins i and j at different locations to have different Larmor frequencies.

In the presence of a background gradient $\omega_i = \gamma(B_0 + Gs_i)$, where s_i is a distance coordinate along the gradient direction. Signal from transverse magnetization terms in Expression [7] which are modulated by sinusoidal functions of absolute position ($\sin(\omega_i + \omega_j)t$ or $\cos(\omega_i + \omega_j)t$), or odd functions of relative position ($\sin(\omega_i - \omega_j)t$), will be averaged to zero (*5*). Signal from terms modulated by even functions of relative position, ($\cos(\omega_i - \omega_j)t$), will not average to zero since all such terms are multiplied by D_{ij}. D_{ij} contains the factor r_{ij}^{-3} ($\mathbf{r}_{ij}$ is the interspin vector) which gives the sinusoids a decay envelope. This ensures that even functions of relative position have a nonzero integral over the sample space.

The $\cos(\omega_i - \omega_j)t$ term only occurs with nonoscillatory factors when $t_2 = 2t_1$. Consider the specific term in Expression [7] associated with the ith spin and modulated by $\cos(\omega_i - \omega_j)t$ when $t_2 = 2t_1$.

$$\tfrac{1}{4}\sum_{j=1}^{N} + I_{xi}\cos(\gamma G t_1(s_i - s_j))\, D_{ij}t_2. \quad [8]$$

Now, ignoring positive constants that scale the signal strength from I_{xi} and assuming all spins in the bulk are equivalent, the sign of the signal from the $n = 2$ pathway will be determined by

$$\int_{\text{volume}} \cos(\gamma G \mathbf{r}\cdot\hat{\mathbf{s}})\, \frac{(3\cos^2\theta - 1)}{r^{-3}}\, r^2\sin^2\theta d\theta d\phi dr. \quad [9]$$

The summation over j from Expression [8] is treated as a sample volume integration (from $r_{\min}$ to the sample boundaries). The center of the coordinate system is taken at $\mathbf{r}_i$ and $\mathbf{s}$ is the gradient direction. Note that the spatial dependence of D_{ij} has been introduced in Expression [9]. Using the result from (*1*) for the solid angle integration, Expression [9] reduces to

$$((3(\hat{\mathbf{s}}\cdot\hat{\mathbf{z}})^2 - 1)) \int_r F(\gamma G t_1 r). \quad [10]$$

The function F contains all r dependence. The integral of F is negative so the phase of the signal depends on the sign of $-[(3(\hat{\mathbf{s}}\cdot\hat{\mathbf{z}})^2 - 1]$. Taking the gradient as being parallel to the polarizing field we find that the phase of the signal will be $-x$. With the gradient perpendicular to the field the phase of the signal is $+x$ and the amplitude is halved. The integral of F is greatest when $\gamma G t_1 r$ ranges between 2 and 4 in a large fraction of the sample (*5*), that is, the gradient imparts to the spins a helical phase-twist with wavelength smaller than sample di-

TABLE 1
Coherence Pathways for MSE Experiment with $\phi_1 = x$, $\phi_2 = x$

nth-Order term from ρ_{eq}	t_1 domain (term at $t = 0$)	$\rightarrow$ (term at $t = t_{1-}$)	t_2 domain (term at $t = t_{1+}$)	$\rightarrow$ (terms at $t = t_1 + t_2$)
$+(\beta\hbar\omega_0)I_{zi}$	$-I_{yi}$	$\rightarrow +I_{xi}\sin(\omega_i t_1)$	$+I_{xi}\sin(\omega_i t_1)$	$\rightarrow +I_{xi}\sin(\omega_i t_1)\cos(\omega_i t_2)$ $+I_{yi}\sin(\omega_i t_1)\sin(\omega_i t_2)$
$+(\beta\hbar\omega_0)^2 I_{zi}I_{zj}$	$+I_{yi}I_{yj}$	$\rightarrow -I_{xi}I_{yj}\sin(\omega_i t_1)\cos(\omega_j t_1)$	$-I_{xi}I_{zj}\sin(\omega_i t_1)\cos(\omega_j t_1)$	$\rightarrow -I_{yi}\sin(\omega_i t_1)\cos(\omega_j t_1)\cos(\omega_i t_2)D_{ij}t_2$ $+I_{xi}\sin(\omega_i t_1)\cos(\omega_j t_1)\sin(\omega_i t_2)D_{ij}t_2$
$+(\beta\hbar\omega_0)^3 I_{zi}I_{zj}I_{zk}$	$-I_{yi}I_{yj}I_{yk}$	$\rightarrow +I_{xi}I_{yj}I_{yk}\sin(\omega_i t_1)\cos(\omega_j t_1)\cos(\omega_k t_1)$	$+I_{xi}I_{zj}I_{zk}\sin(\omega_i t_1)\cos(\omega_j t_1)$ $\times \cos(\omega_k t_1)$	$\rightarrow -I_{xi}\sin(\omega_i t_1)\cos(\omega_j t_1)\cos(\omega_k t_1)$ $\times \cos(\omega_i t_2)D_{ij}D_{ik}(t_2)^2$ $-I_{yi}\sin(\omega_i t_1)\cos(\omega_j t_1)\cos(\omega_k t_1)$ $\times \sin(\omega_i t_2)D_{ij}D_{ik}(t_2)^2$
$+(\beta\hbar\omega_0)^4 I_{zi}I_{zj}I_{zk}I_{zl}$	$+I_{zi}I_{zj}I_{zk}I_{zl}$	$\rightarrow -I_{xi}I_{yj}I_{yk}I_{yl}\sin(\omega_i t_1)\cos(\omega_j t_1)\cos(\omega_k t_1)$ $\times \cos(\omega_l t_1)$	$-I_{xi}I_{zj}I_{zk}I_{zl}\sin(\omega_i t_1)\cos(\omega_j t_1)$ $\times \cos(\omega_k t_1)\cos(\omega_l t_1)$	$\rightarrow +I_{yi}\sin(\omega_i t_1)\cos(\omega_j t_1)\cos(\omega_k t_1)$ $\times \cos(\omega_i t_1)\cos(\omega_i t_2)D_{ij}D_{ik}D_{il}(t_2)^3$ $-I_{xi}\sin(\omega_i t_1)\cos(\omega_j t_1)\cos(\omega_k t_1)$ $\times \cos(\omega_i t_1)\sin(\omega_i t_2)D_{ij}D_{ik}D_{il}(t_2)^3$

mensions but larger than r_{min}. In such cases (with a strong polarizing field) the signal from a water sample at $t_2 = 2t_1$ will be a sizable fraction of the primary echo (*5*).

We extend the preceding arguments to the third- and fourth-order pathways. The coherence pathways when $\phi_1 = x$, $\phi_2 = x$ are shown in Table 1. Signal timing and phase calculations remain remarkably simple for $n > 2$ because of spatial averaging. For $n = 3$ terms at $t_2 = 3t_1$ we have the observable (dropping positive constants)

$$\sum_{i=1}^{N}\sum_{j=1}^{N}\sum_{k=1}^{N} -I_{yi}\cos(\omega_i - \omega_j + \omega_i - \omega_k)\,D_{ij}D_{ik}. \quad [11]$$

This is the only transverse magnetization from the $n = 3$ pathway which is modulated by an even function of relative position. By using a standard identity

$$\cos(\omega_i - \omega_j + \omega_i - \omega_k) = \tfrac{1}{2}[\cos(\omega_i - \omega_j)\cos(\omega_i - \omega_k) + \sin(\omega_i - \omega_j)\sin(\omega_i - \omega_k)], \quad [12]$$

and noting that signal from sine modulated terms averages to zero, the observable term associated with a specific ith spin can be written

$$-I_{yi}N\{\sum_{j=1}^{N}\cos(\omega_i - \omega_j)\,D_{ij}\}\{\sum_{k=1}^{N}\cos(\omega_i - \omega_k)\,D_{ik}\}. \quad [13]$$

The phase of the signal is now determined by $[-((3(\hat{\mathbf{s}}\cdot\hat{\mathbf{z}})^2 - 1)]^2$ which is always positive. The phase of the echo at $t_2 = 3t_1$ is $-y$ regardless of the gradient direction.

As a final example we consider the observable on the $n = 4$ pathway at $t_2 = 4t_1$,

$$\sum_{i=1}^{N}\sum_{j=1}^{N}\sum_{k=1}^{N}\sum_{l=1}^{N} -I_{xi}\cos(\omega_i - \omega_j + \omega_i - \omega_k + \omega_i - \omega_l)\,D_{ij}D_{ik}D_{il}. \quad [14]$$

The term associated with a specific ith spin reduces to

$$-I_{xi}\{\sum_{j=1}^{N}\cos(\omega_i - \omega_j)\,D_{ij}\}\{\sum_{k=1}^{N}\cos(\omega_i - \omega_k)\,D_{ik}\} \times \{\sum_{l=1}^{N}\cos(\omega_i - \omega_l)\,D_{il}\} \quad [15]$$

so that the signal phase at $t_2 = 4t_1$ depends on the sign of $[-((3(\hat{\mathbf{s}}\cdot\hat{\mathbf{z}})^2 - 1)]^3$. Therefore the phase is $+x$ when the gradient is parallel to the polarizing field.

A summary of these results is found in Table 2a. A similar table of coherence pathways can be constructed for $\phi_1 = x$, $\phi_2 = y$. The summation of signals is carried out in the same way. The phase predictions for successive echoes for the 90_x 90_y experiment are summarized in Table 2b.

Several important points about the MSE experiment are apparent from the density matrix calculations:

(i) Changing $\hat{\mathbf{s}}\cdot\hat{\mathbf{z}}$ from 1 to 0 changes the sign of even echoes by 180°.

(ii) Changing ϕ_1 from x to $-x$ introduces a sign change in odd order pathways; as a result the sign of odd echoes is changed by 180°. Therefore, in contrast to conventional expectation based on an initial thermal equilibrium state of single I_z polarization, signal will be seen when the results of a 90_x 90_x experiment are added to that of a 90_{-x} 90_x experiment.

(iii) Modulation terms for an nth-order pathway can only become a function of relative position at $t_2 = nt_1$ and therefore

TABLE 2
Summary of Phase Predictions

(a) $\phi_1 = \pm x$, $\phi_2 = x$

n	$(90_x, 90_x)$ $\hat{\mathbf{s}} \cdot \hat{\mathbf{z}} = 1$	$(90_{-x}, 90_x)$ $\hat{\mathbf{s}} \cdot \hat{\mathbf{z}} = 1$	$(90_x, 90_x)$ $\hat{\mathbf{s}} \cdot \hat{\mathbf{z}} = 0$	$(90_{-x}, 90_x)$ $\hat{\mathbf{s}} \cdot \hat{\mathbf{z}} = 0$
1	$+y$	$-y$	$+y$	$-y$
2	$-x$	$-x$	$+x$	$+x$
3	$-y$	$+y$	$-y$	$+y$
4	$+x$	$+x$	$-x$	$-x$

(b) $\phi_1 = \pm x$, $\phi_2 = y$

n	$(90_x, 90_y)$ $\hat{\mathbf{s}} \cdot \hat{\mathbf{z}} = 1$	$(90_{-x}, 90_y)$ $\hat{\mathbf{s}} \cdot \hat{\mathbf{z}} = 1$	$(90_x, 90_y)$ $\hat{\mathbf{s}} \cdot \hat{\mathbf{z}} = 0$	$(90_{-x}, 90_y)$ $\hat{\mathbf{s}} \cdot \hat{\mathbf{z}} = 0$
1	$-y$	$+y$	$-y$	$+y$
2	$+y$	$+y$	$-y$	$-y$
3	$-y$	$+y$	$-y$	$+y$
4	$+y$	$+y$	$-y$	$-y$

the time domain order of multiple echoes is the same as the quantum coherence order that causes the echo.

(iv) The observable higher order echo signals arise entirely from the action of the dipolar field following the second 90° pulse. During the interval between the two 90° pulses the role of the dipolar interaction is to generate terms in the density matrix which remain unobservable over all subsequent evolution. Hence no importance need be attached to the precise temporal positioning of the gradient pulses used for coherence transfer selection in the CRAZED experiment, Fig. 1b.

(v) The MSE experiment can be thought of as a superposition of CRAZED experiments ($n = 1, 2, 3 \ldots$ in Fig. 1b). When one compares gradient area in the t_1 domain to gradient area in the t_2 domain for a MSE experiment one finds that a 1:1 ratio exists at $t_2 = t_1$ (cf., Fig. 1b, $n = 1$), 1:2 ratio exists at $t_2 = 2t_1$ (cf., Fig. 1b, $n = 2$) and so forth. Hence the nth-order MSE echo is equivalent to the signal from the nth CRAZED experiment.

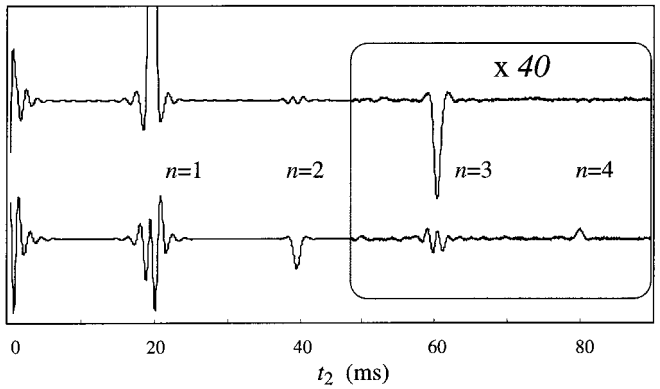

FIG. 2. Time domain signals from the MSE experiment (Fig. 1a) $\phi_1 = x$, $\phi_2 = x$, $t_1 = 20$ ms, $G = 0.4$ G/cm. The upper line is the imaginary channel, and the lower line is the real channel. Data within the box are magnified 40 times.

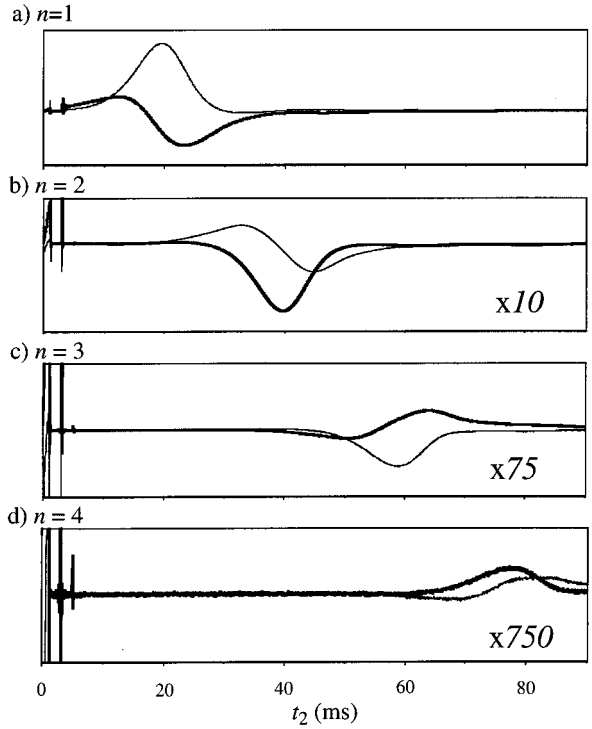

FIG. 3. Time domain signals from nth-order CRAZED experiment (Fig. 1b). $\phi_1 = x$, $\phi_2 = x$, $t_1 = 20$ ms, $T = 2$ ms. The thick line is the real channel data, and the thin line is the imaginary channel data. Magnification relative to (a) is shown in (b) through (d).

EXPERIMENTAL

In order to demonstrate their equivalence, we have performed both CRAZED and MSE experiments on a cylindrical sample of 5000 Da polydimethylsiloxane (PDMS) at 7 T (300 MHz ^{1}H NMR frequency). A 10-mm-diameter NMR tube was used with a length of sample greater than that of the RF coil (12 mm), so as to avoid susceptibility effects near the air/polymer

TABLE 3

(a) Phase Cycle Selection of $n = 1$ Echo

ϕ_1	$+x$	$-x$	$+x$	$-x$
ϕ_2	$+x$	$+x$	$+y$	$+y$
Acquisition phase	$+x$	$-x$	$-x$	$+x$

(b) Phase Cycle Selection of $n = 2$ Echo

ϕ_1	$+y$	$-y$	$+x$	$-x$
ϕ_2	$+y$	$+y$	$+y$	$+y$
Acquisition phase	$+x$	$+x$	$-x$	$-x$

(c) Phase Cycle Selection of $n = 3$ Echo

ϕ_1	$+x$	$-x$	$-x$	$+x$
ϕ_2	$+x$	$+x$	$+y$	$+y$
Acquisition phase	$+x$	$-x$	$-x$	$+x$

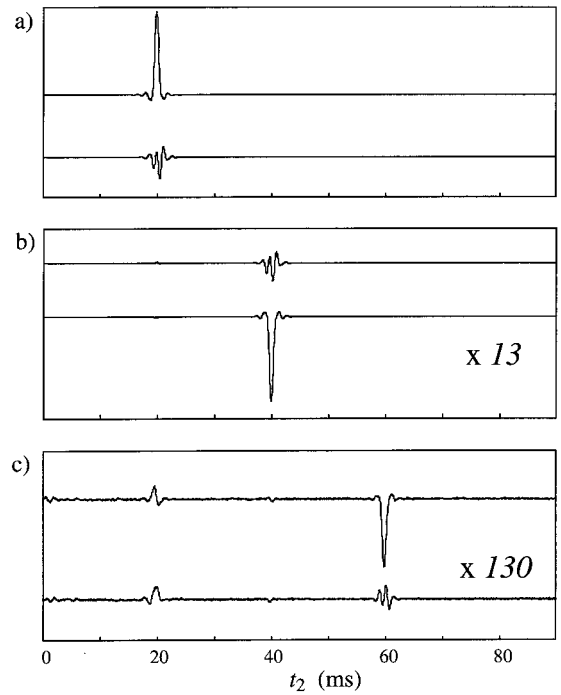

FIG. 4. Time domain signals from the MSE experiment (Fig. 1a) using phase cycling to select successive echo orders. The upper lines are the imaginary channel, and the lower lines are the real channel. The phase cycles select (a) the first-order echo, (b) the second-order echo, (c) the third-order echo. Phase cycles are shown in Tables 3a to 3c, respectively. Magnification relative to the first-order echo is shown in (b) and (c).

interface. The choice of the PDMS sample ensures a high proton density, comparable with that of water, but a small cutoff length ($r_{\min}$) since the diffusion coefficient of these molecules is at least one order of magnitude less than that of water. The results of the MSE experiment, performed using a steady magnetic field gradient, are shown in Fig. 2, where echo orders out to 4 are clearly observable. Figures 3a to 3d show the corresponding CRAZED time domain signals. Gradient pulse area ratios are varied from 1 to 4; the correspondence between the echo order in Fig. 2 and the multiple quantum coherence transfer order in Figs. 3a to 3d is clearly apparent. The CRAZED signals are much broader in the time domain than the corresponding MSE signals because no steady background gradient is needed when CRAZED signals are acquired.

Table 2 indicates that phase discrimination is possible between signals from $n = 1$ to 4. Suppose we wish to keep only the first-order echo in an MSE experiment and suppress $n = 2$, 3, 4. For this purpose the phase cycle shown in Table 3a is effective and the result is shown in Fig. 4a. Figures 4b and 4c show the results of phase cycles that select $n = 2$ and 3, respectively, while suppressing other orders. Figure 4c shows that about 0.1% of the first echo has leaked through, this small fraction indicates a high degree of suppression.

Finally we note that when the angle between **s** and **z** is set to the magic angle, the symmetry-breaking effects of the magnetic field gradient are minimized. All remaining dipolar field effects must arise from the sample shape alone. As has been observed previously (*4*), we also find that the use of a magic-angle gradient results in a significant reduction of the amplitude of the higher order echoes in the MSE experiment.

DISCUSSION

The phase cycle selection of $n = 1$ echoes which has been demonstrated here may prove useful as a technique for suppressing solvent artifacts in COSY spectroscopy experiments. It may also be used to suppress artifacts in imaging experiments where background gradients and gradient pulses are used.

The different signal phases of $90_x\ 90_x$ and $90_x\ 90_y$ MSE experiments have been known for some time (*4*); however, it has not been previously noted that these phases differences are incompatible with the HTA. By using density matrix theory we have been able to calculate the phase and timing of MSE echoes from all possible quadrature phase combinations of ϕ_1 and ϕ_2. As a result we have been able to devise phase cycles which select each of the orders $n = 1$ to $n = 4$. We emphasise that such phase cycling would not be possible if the initial state of the density matrix comprised only linear terms of the form I_{zi}. The experimental confirmation (Figs. 4a to 4c) of theoretical phase predictions provides a convincing demonstration that the higher order coherences in the CRAZED and MSE experiments must arise directly from corresponding higher order I_z spin operator products in ρ_{eq}.

REFERENCES

1. G. Deville, M. Bernier, and J. M. Delrieux, *Phys. Rev. B* **19,** 5666 (1979).
2. D. Einzel, G. Eska, Y. Hirayoshi, T. Kopp, and P. Wolfle, *Phys. Rev. Lett.* **53** 2312 (1984).
3. W. Durr, D. Hentschel, R. Ladebeck, R. Oppelt, and A. Oppelt, Abstracts, of the Society of Magnetic Resonance in Medicine, 8th Annual Meeting, p. 1173 (1989).
4. R. Bowtell, R. M. Bowley, and P. Glover, *J. Magn. Reson.* **88,** 643 (1990).
5. W. S. Warren, W. Richter, A. H. Andreotti, and B. T. Farmer, *Science* **262,** 2005 (1993).
6. S. Lee, W. Ricter, S. Vathyam, and W. S. Warren, *J. Chem. Phys.* **105,** 874 (1996).
7. J. Jeener, A. Vlassenbroek, and P. Broekaert, *J. Chem. Phys.* **103,** 1309 (1995).
8. M. H. Levitt, *Concepts Magn. Reson.* **8,** 77 (1996).
9. W. S. Warren, S. Lee, W. Richter, and S. Vathyam, *Chem. Phys. Lett.* **247,** 207 (1995).
10. A. Abragam, "Principles of Nuclear Magnetism," Clarendon Press, Oxford (1961).
11. R. R. Ernst, G. Bodenhausen, and A. Wokaun, "Principles of NMR in One and Two Dimensions," Oxford Univ. Press, Oxford (1987).